Nano World Journal

https://doi.org/10.17756/nwj.2023-s4-072

Research Article

Open Access

Finite Element Solution for Thermal Radiation, and Viscous Dissipation Affected Vertical Plate in Blended Convective Micropolar Fluid Flow

T. Lokesh Babu[1,2*], S.V.H.N. Krishna Kumari[2] and M.N. Rajasekar[3]

[1]*Department of Mathematics, Sreenidhi Institute of Science and Technology, Hyderabad, Telangana, India*

[2]*Department of Mathematics, Vardhaman College of Engineering, Hyderabad, Telangana, India*

[3]*Department of Mathematics, College of Engineering, JNT University, Hyderabad, Telangana, India*

***Correspondence to:**
T. Lokesh Babu
Department of Mathematics,
Sreenidhi Institute of Science and Technology,
Hyderabad, Telangana, India.
E-mail: lokeshbabut@sreenidhi.edu.in

Department of Mathematics,
Vardhaman College of Engineering,
Hyderabad, Telangana, India.

Received: September 19, 2023
Accepted: November 29, 2023
Published: December 04, 2023

Citation: Babu TL, Kumari SVHNK, Rajasekar MN. 2023. Finite Element Solution for Thermal Radiation, and Viscous Dissipation Affected Vertical Plate in Blended Convective Micropolar Fluid Flow. *NanoWorld J* 9(S4): S427-S434.

Published by United Scientific Group

Abstract

The investigation is directed to illustrate the thermal radiation's impact on emphatical blended convection stream of micropolar incompressible viscous fluid. In which, by using both viscous thermal dissipation and advanced wave class of radial disturbance, the vertical porous plate of a semi-infinite class is investigated. Generally, the well-known Roseland approximation is taken to analyze the thermal transfer in various optically thick viscous streams, and which is also implemented for the current investigation. The non-linear group of partial differential equations will transform the non-dimensional set of equations involved. Variables that are not dimensional the equations in non-dimensional form solved numerically with the help of various finite element methods is a more economical way in computational view. The other quantitate such as friction and heat transfer in the stream was also evaluated through the graphs drawn. All the numerical evolutions, including linear and angular fluids, are differentiated and papalized with the stream problems for a Newtonian fluid.

Keywords

Viscous dissipation, Blended convection, Finite element approach, Thermal radiation, Micropolar fluid, Nanotechnology.

Nomenclature

x' - Horizontal distance on plate; y' - Perpendicular distance on plate; t' - Time (dimensional); g - Acceleration due to gravity; u' - Velocity (dimensional); T_w' - Temperature around at wall; p' - Thermo dynamic pressure; T_∞' - Far away temperature; j' - Micro-inertia (dimensional); q_r - Heat flux; k^* - Mean absorption coefficient; u - Horizontal velocity component; y - Depth; t - Time (non-dimensional); U_∞ - Free stream (non-dimensional) velocity; u_p - Plate velocity (dimensional); C_f - Skin-friction coefficient; j - Micro-inertia (non-dimensional); Pr - Prandtl number; C_p - Specific heat; R - Radiation parameter; Nu - Nusselt number; Ec - Eckert number; Gr - Grashof number; U_p - Plate velocity (non-dimensional); B_o - magnetic field; ρ - Density; α - Thermal diffusivity; v - Kinematic viscosity; ω' - Angular velocity (dimensional); κ - Thermal conductivity; δ - Frequency (non-dimensional); μ - Dynamic viscosity; β^* - Coefficient of volumetric expansion; ω - Angular velocity vector; ε - Scalar constant (≤ 1); θ - Temperature (non-dimensional); v_r - Fluid kinematic rotational viscosity; $\overline{\sigma}$ - Stefan-Boltzmann constant; v - Perpendicular velocity component; T' - Temperature (dimensional); n' - Frequency of oscillation; ' – Differentiation; w - Wall condition; ∞ - Free Stream Condition.

Introduction

Generally, various classes of streams which exhibit microscopic characteristics originate from the micromotions of the different fluid components are described in a subject of micropolar streams (or) fluids. The streams (or) fluids of these classes exhibit spin inertia due to the involvement of rigid macromolecules (dilute suspension), which further leads to fluid stress and steam body moments. Typically, non-Newtonian streams are a class of micropolar fluids containing the overall hydrodynamics of the stream can change as a result of rotating micro-components. Detailed analysis and ideas on micro-rotation and its derivatives such as various frequency parameters of micropolar unsteady flow of stream between parallel porous plates given by Srinivasacharya et al. [1]. Similar analysis was also done by Bhargava et al. [2], in which all the numerical solutions of MHD micropolar streamflow were studied between parallel plates using a quasi-linearization procedure. Velocity components and temperature of the nanoparticles are influenced significantly by the inclusion of nanoparticles. Heat enhancement is observed when copper and silver nonmagnetic nanoparticles are used instead of simple base fluid (conventional fluid). The radiative nature of nano-plasma in the presence of magnetic field causes a decrease. Influence of all the dimensionless quantities which randomly occur in the current research, which include various linear and angular velocity parameters and inclusive temperature profiles across the edges of the steam layers. The hydromagnetic flow of steam (micropolar) between parallel walls of porous nature was examined by the authors Zueco et al. [3], in which network simulation methodology was adopted. In their analysis, all the authors addressed magnetic field origin and its importance in monitoring changes of heat transfer in MHD usage and its applications. The latest investigation by Sheikholeslami et al. [4] advises the homotopy perturbation procedure, which includes different chemical reactions involved in the micropolar fluid flow of the present kind. The author, Cheng [5], described different closed-form analytic solutions of micropolar fluids by using vertical channels in which he studied heat transfer characteristics of the stream. Recent research by Kumar et al. [6] addressed fully enriched convective stream in vertical channel covered with the micropolar stream. The authors, Umavathi and Sultana [7], introduced a similar subject in which they have discussed and developed an utterly blended convection flow of micropolar stream blend in a vertical channel by using homotopy and differential transform procedure. And they have been evaluated different characteristics of a micropolar fluid, which are found to be lower grades than Newtonian steam. Under various boundary conditions, different heat moments in micropolar streams are described by Rahman et al. [8]. In such a way, quite another side, heat transfer in blended or free convection and thermal radiation at the same instant, particularly in the case of the micropolar stream has not gained much attention. There is a lot of scope in this direction as an investigation of thermal radiation, which plays a crucial role in evaluating total surface effects in terms of heat transfer at various instants, which will be most helpful in space technology. Mahmoud [9] explained the effects of the magnetic field, changes in thermal radiation, and conductivity inflow of an electrically sustained micropolar stream over a stretching surface with a temperature change. Nanotechnology involves manipulating matter on an atomic or molecular scale, typically at the nanometer scale. It's a multidisciplinary field that merges science and engineering, aiming to understand, control, and utilize materials and devices at the nanoscale.

In his research, the temperature relative to a surface was assumed to vary under a power law. Energy, linear, and angular momentum in equation form is transformed into the non-linear differential equation using similarity transformation. The author, Prasad et al. [10], are given a mathematical analysis for horizontally conducting dense streams. In which they have studied embedded isothermal permeable spheres in different porosity mediums. They have also simulated non-darcy effects employing second-order forchheimer drag force by using boundary equation. The conservative equations related to all the boundaries observed to be parabolic are changed into non-similar forms. And which are further solved by Keller Box (finite difference) scheme. Similar ideas were also discussed by both Palani and Kim [11], in which they have been analyzed the effect of surface heat flux on vertical cone in convection stream. Mahmoud and Waheed [12] also done parallel work, in which they have studied slip velocity of flat plate affected with thermal radiation in a convection stream. Oahimire and Olajuwon [13] studied heat and mass transfer influence chemically reacting (unsteady) stream over a porous plate in a magnetic field. They have also verified the Hall effect and corresponding parameters. In their research, various perturbation techniques were used to translate partial differential equations into non-dimensional equations. Investigated is the movement of a semi-infinite vertical porous plate by a viscous, incompressible micropolar fluid. The authors, Kim and Fedorov [14] represented solutions of equations about Laplace transform techniques. In which they have studied in detail free stream progressive wave disturbance. All the studies do not explain well about viscous dissipation in detail studies as mentioned earlier. Various applications characterized by Eckert numbers, such as geophysical flows and their industrial derivatives, are greatly influenced by the effect of viscous dissipation. Rahman [15] described laminar steady convective free stream. Micropolar streams and heat transfer include Joule heating, isothermal absorbent layers, and viscous dissipations. Buoyancy force and viscous dissipation in heated vertical layers of the incompressible. Mircopolar non-uniform blended streams were well explained by Abd El-Aziz [16]. Dissipation, dispersion, and Joule heating effects in free MHD convection stream and a presence of magnetic field explained by El-Hakeem [17]. Using the Chebyshev (finite difference) method, Ohmic heating, dissipation (viscous) of hydromagnetic stream, and its numerical solutions were discussed in Eldabe and Ouaf [18]. Effects and perturbation analysis on thermal irradiated Newtonian stream saturated in a porous medium concerning Newtonian streamflow was studied by Rashad [19]. Within constant temperature periodic variation non-Newtonian flow explained by Eldabe et al. [20]. In which mass and heat transfer were studied through Eyring-Powell stream in the porous material. Current research aims to resolve a problem in which thermally irradiated steadily traveled porous plate opted for a change in suction velocity under mixed convection stream of a micropolar fluid. Here the micropolar stream adopted is a

non-scattered and optically thick channel. In which radiative heat flux is explained with the help of Rosseland approach. We also consider the impact of the viscous dissipation and the uniform transverse magnetic field. Once the stream equations are transformed into non-linear equations, the finite element differential approach is used to resolve the specified issue, and corresponding parameters skin-friction and rate of heat transfer are obtained. Hence, in this direction, the present research aimed to make the best mathematical modeling towards the selected problem and its usefulness in fluid dynamics.

Experimentation

Mathematical formulation

Figure 1 represents the general coordinates and the study's physical problem model. In the current investigation, we have assumed a 2-dimensional unsteady free convection stream of incompressible tiny polar fluid. In which thermally irradiated vertical plates (semi-infinite) without magnetic field influence have been chosen for analysis. For better analysis, the *x*' - axis is chosen for the upward direction along with the vertical plate, and the *y*' - axis is chosen for regular happening with the vertical plate. The acceleration is due to gravity held in a direction that is opposite to the *x*' - variable. The following restrictions are assumed to be implanted in the current research problem. (i) Excluding density, all the other fluid characteristics in buoyancy force are stable and constant, (ii) Under critical energy conservation, equations concerning heat and viscous dissipation are included to resolve the present problem, (iii) Reynolds number (Magnetic) assumed too small and neglected, and (iv) In comparison to the typical length scale of a micropolar stream, the diameters of the holes in the porous plate were thought to be excessively large.

Based on the assumptions made, the following equations, including linear and angular momentum, mass, and energy conservation, can be addressed in the cartesian frame of reference.

The continuity equation indicates (1)

as per the liner momentum equation

$$\frac{\partial u'}{\partial t'}+v'\frac{\partial u'}{\partial y'}= -\frac{1}{\rho}\frac{\partial p'}{\partial x'}+\left(\nu+\nu_r\right)\frac{\partial^2 u'}{\partial y'^2}+g\beta^*\left(T'-T_\infty'\right)+2\nu_r\left(\frac{\partial \omega'}{\partial y'}\right) \quad (2)$$

as per the angular momentum equation

$$\frac{\partial \omega'}{\partial t'}+v'\frac{\partial \omega'}{\partial y'}=\left[\frac{\gamma}{\rho j'}\right]\frac{\partial^2 \omega'}{\partial y'^2} \quad (3)$$

as per the energy equation

$$\frac{\partial T'}{\partial t'}+v'\frac{\partial T'}{\partial y'}=\alpha\left(\frac{\partial^2 T'}{\partial y'^2}-\frac{\partial q_r}{\partial y'}\right)+\frac{\nu}{C_p}\left(\frac{\partial u'}{\partial y'}\right)^2 \quad (4)$$

The radiative heat flux in the *y*' direction, as per Roseland approximation is given as follows. For the time being, only optically dense streams are considered. if it treads under Roseland approximation. For a small temperature range, the above equation can be linearized in turns of Taylor series expansion and in which all higher-order terms (T'^4 into the about T_∞') are given as follows.

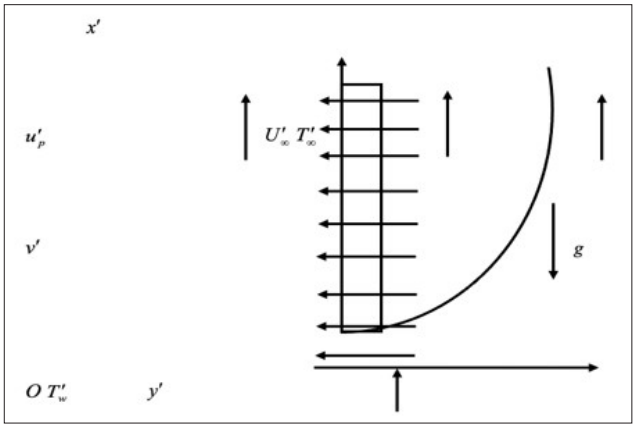

Figure 1: Representation of co-ordinate system and physical model of problem.

$$T'^4 \cong 4T_\infty'^3 T'-3T_\infty'^4 \quad (5)$$

Viscous dissipation is assumed to be small by heating; small velocities in the equation 2 of energy conservation, which leads to variation in equation 2 and further, which is described employing Boussinesq's approximation. Here the assumption is exponentially increasing (or) decreasing the stream velocity, suction velocity, and plate temperature has been taken, and perturbation theory implemented to resolve the problem. By implementing appropriate boundary conditions and assumptions made, the variation in velocity, micro-rotation, and temperature fields are given by.

$$q_r=-\frac{4\bar{\sigma}}{3k^*}\frac{\partial T'^4}{\partial y'} \quad (6)$$

$$t'\le 0;\quad u'=0,\quad \omega'=0,\quad T'=T_\infty' \text{ for all } y'$$

$$t'>0:\begin{cases} u'=u_p',\ \omega'=-n'\dfrac{\partial u'}{\partial y'},\ T'=T_w'+\varepsilon\left(T_w'-T_\infty'\right)e^{n't'} \text{ at } y'=0 \\ u'=U_\infty'=U_0\left(1+\varepsilon e^{n't'}\right),\ \omega'\to 0,\ T'\to T_\infty' \text{ at } y'\to\infty \end{cases} \quad (7)$$

The variable ω' in equation 7 describes the relation with surface stress, including micro-rotation within the fluid. In this expression, the quantity *n*' is a number that ranges from 0 to 1 and relates the micro-gyration to shear stress. If the value of the *n*' approach is zero, including the large density leads to slow rotational around at the boundaries of the vertical plate.

Higher values in steps like 0.5 and 1 are indicative of weak and turbulent boundary layers.

based on analysis and boundaries outside of the wall (2) is reduced to:

$$-\frac{1}{\rho}\left(\frac{dp'}{dx'}\right)=\frac{dU_\infty'}{dt'} \quad (8)$$

To resolve the problem, let us introduce dimensionless quantities, which are given as follows.

$$\left.\begin{aligned} u=\frac{u'}{U_o},v=\frac{v'}{V_o},y=\frac{V_o y'}{\nu},t=\frac{t'V_o^2}{\nu},U_\infty=\frac{U_\infty'}{U_o},U_p=\frac{u_p'}{U_o} \\ \omega=\frac{\nu}{U_oV_o}\omega',\theta=\frac{T'-T_\infty'}{T_w'-T_\infty'},\delta=\frac{n'\nu}{V_o^2},j^*=\frac{V_o^2}{\nu^2}j',\mathrm{Pr}=\frac{\nu\rho C_p}{\kappa}=\frac{\nu}{\alpha}, \\ Gr=\frac{\nu g\beta^*\left(T_w'-T_\infty'\right)}{U_oV_o^2},R=\frac{\kappa k^*}{4\sigma T_\infty'^3},Ec=\frac{V_o^2}{C_p\left(T_w'-T_\infty'\right)} \end{aligned}\right\} \quad (9)$$

After that, spin-gradient viscosity, which describes the correlation between the co-efficient of micro-inertia and viscosity, is given as follows.

$$\gamma=\left(\mu+\frac{A^*}{2}\right)j'=\mu j'\left(1+\frac{\beta}{2}\right) \quad (10)$$

Where, β defined as $\beta=\frac{A^*}{\mu}$ (11)

Where β is the gyro-viscosity coefficient. In such a way, the equation 8 to 11.

$$\frac{\partial u}{\partial t}-\left(1+\varepsilon Ae^{\delta t}\right)\frac{\partial u}{\partial y}= \frac{dU_\infty}{dt}+\left(1+\beta\right)\frac{\partial^2 u}{\partial y^2}+\left(Gr\right)\theta+2\beta\left(\frac{\partial\omega}{\partial y}\right) \quad (12)$$

$$\frac{\partial\omega}{\partial t}-\left(1+\varepsilon Ae^{\delta t}\right)\frac{\partial\omega}{\partial y}=\frac{1}{\eta}\frac{\partial^2\omega}{\partial y^2} \quad (13)$$

$$\frac{\partial\theta}{\partial t}-\left(1+\varepsilon Ae^{\delta t}\right)\frac{\partial\theta}{\partial y}= \frac{1}{\mathrm{Pr}}\left(1+\frac{4}{3R}\right)\frac{\partial^2\theta}{\partial y^2}+Ec\left(\frac{\partial u}{\partial y}\right)^2 \quad (14)$$

Where, $\eta=\frac{\mu j'}{\gamma}=\frac{2}{2+\beta}$.

Represented equation 7, which describes the boundary conditions, are taken following the dimensionless form $t \le 0$: $u = 0, \omega = 0, \theta = 0$ for all y.

Given t > 0: $\left.\begin{aligned} u=U_p,\frac{\partial\omega}{\partial y}=-\delta\frac{\partial u}{\partial y},\theta=1+\varepsilon e^{\delta t}\ at\ y=0 \\ u\to U_\infty,\ \omega\to 0,\ \theta\to 0 \text{ as } y\to\infty \end{aligned}\right\}$ (15)

Nomenclature indicates all the meanings of various parameters. In this view, equation 12 to 14 describe the velocity variations, micro-rotation, and temperature around the boundary layer. All the allowed to calculate the skin friction coefficient of the porous plate. The following equation represents such an analysis.

$$C_f=\frac{\tau_w^*}{\rho U_oV_o}=\left[\frac{\partial u}{\partial y}\right]_{y=0} \quad (16)$$

In this solving process, we can also evaluate the co-efficient of heat transfer in terms of Nusselt number, which is given as follows.

$$Nu=\left(1+\frac{4}{3R}\right)\frac{x'}{\left(T_w'-T_\infty'\right)}\left[\frac{\partial T'}{\partial y'}\right]_w\Rightarrow Nr\,\mathrm{Re}_x^{-1}=-\left(1+\frac{4}{3R}\right)\left[\frac{\partial\theta}{\partial y}\right]_{y=0} \quad (17)$$

Where, $\mathrm{Re}_x^{-1}=\frac{V_o x'}{\nu}$ is Reynolds number.

Method of solution by finite element technique

Equation 12 initiated with Galerkin Technique (finite element) over the element (e), $(y_j \le y \le y_k)$ is:

$$\int_{y_i}^{y_k}\left\{N^T\left[\left(1+\beta\right)\frac{\partial^2 u^{(e)}}{\partial y^2}+Z\frac{\partial u^e}{\partial y}-\frac{\partial u^e}{\partial t}+p\right]\right\}dy=0 \quad (18)$$

Where, $Z=1+\varepsilon Ae^{\delta t},P=\frac{dU_\infty}{dt}+\left(Gr\right)\theta^{(e)}+2\beta\left(\frac{\partial\omega^{(e)}}{\partial y}\right)$;

The result of integrating the first term in equation 18.

$$N^{(e)^T}\left(1+\beta\right)\left\{\frac{\partial u^e}{\partial y}\right\}-\int_{y_j}^{y_k}\left\{\left(1+\beta\right)\left(\frac{\partial N^{(e)^T}}{\partial y}\right)\left(\frac{\partial u^e}{\partial y}\right)+N^{(e)^T}\left(\left(\frac{\partial u^e}{\partial t}\right)+Z\frac{\partial u^e}{\partial y}-p\right)\right\}dy=0 \quad (19)$$

Ignoring the first term in equation 19, results:

$$\int_{y_j}^{y_k}\left(1+\beta\right)\left(\frac{\partial N\left(e^T\right)}{\partial y}\right)\left(\frac{\partial u^{(e)}}{\partial y}\right)+N^{e^T}\left(\left(\frac{\partial u^{(e)}}{\partial t}\right)+z\left(\frac{\partial u^{(e)}}{\partial y}\right)-p\right)dy=0 \quad (20)$$

Let $u^{(e)} = N^{(e)}\,\phi^{(e)}$ be the solution over the element (e), $(y_j \le y \le y_k)$, where $N^{(e)} = [N_j\ N_k]$, $\phi^{(e)} = [u_j\ u_k]^T$ and $N_j=\frac{y_k-y}{y_k-y_j}$, $N_k=\frac{y-y_j}{y_k-y_j}$ are the basis functions one can get;

$$\int_{y_j}^{y_k}\left(1+\beta\right)\left\{\begin{bmatrix}N_j' & N_j' \\ N_j' & N_k'\end{bmatrix}\begin{bmatrix}u_j \\ u_k\end{bmatrix}\right\}dy+\int_{y_j}^{y_k}\left\{\begin{bmatrix}N_j & N_j \\ N_j & N_k\end{bmatrix}\begin{bmatrix}\dot{u}_j \\ \dot{u}_k\end{bmatrix}\right\}dy+ Z\int_{y_j}^{y_k}\left\{\begin{bmatrix}N_j & N_j' \\ N_j & N_k'\end{bmatrix}\begin{bmatrix}u_j \\ u_k\end{bmatrix}\right\}dy=P\int_{y_j}^{y_k}\begin{bmatrix}N_j \\ N_k\end{bmatrix}dy$$

Simplifying,

$$\frac{\left(1+\beta\right)}{l^{(e)^2}}\begin{bmatrix}1 & -1 \\ -1 & 1\end{bmatrix}\begin{bmatrix}u_j \\ u_k\end{bmatrix}+\frac{1}{6}\begin{bmatrix}2 & 1 \\ 1 & 2\end{bmatrix}\begin{bmatrix}\dot{u}_j \\ \dot{u}_k\end{bmatrix}+\frac{Z}{2l^{(e)}}\begin{bmatrix}-1 & 1 \\ -1 & 1\end{bmatrix}\begin{bmatrix}u_j \\ u_k\end{bmatrix}=\frac{P}{2}\begin{bmatrix}1 \\ 1\end{bmatrix}$$

Grouping the equations for two serial elements $y_{i-1} \le y \le y_i$ and $y_i \le y \le y_{i+1}$ the following results obtained.

$$\frac{\left(1+\beta\right)}{l^{(e)^2}}\begin{bmatrix}1 & -1 & 0 \\ -1 & 2 & -1 \\ 0 & -1 & 1\end{bmatrix}\begin{bmatrix}u_{i-1} \\ u_i \\ u_{i+1}\end{bmatrix}+\frac{1}{6}\begin{bmatrix}2 & 1 & 0 \\ 1 & 4 & 1 \\ 0 & 1 & 2\end{bmatrix}\begin{bmatrix}\dot{u}_{i-1} \\ \dot{u}_i \\ \dot{u}_{i+1}\end{bmatrix}+\frac{Z}{2l^{(e)}}\begin{bmatrix}-1 & 1 & 0 \\ -1 & 0 & 1 \\ 0 & -1 & 1\end{bmatrix}\begin{bmatrix}u_{i-1} \\ u_i \\ u_{i+1}\end{bmatrix}=\frac{P}{2}\begin{bmatrix}1 \\ 2 \\ 1\end{bmatrix} \quad (21)$$

Now, set the row associated with the node i to zero, from equation 21 the difference schemes $I^{(e)} = h$ is:

$$\frac{(1+\beta)}{h^2}\left[-u_{i-1}+2u_i-u_{i+1}\right]+\frac{1}{6}\left[\dot{u}_{i-1}+4\dot{u}_i-\dot{u}_{i+1}\right]+\frac{z}{2h}\left[-u_{i-1}+u_{i+1}\right]=p \quad (22)$$

By using the Crank-Nicholson method to equation 22 and the trapezoidal rule, the following system of equations is derived:

$$A_{1u_{i-1}^{n+1}}+A_{2u_i^{n+1}}A_{3u_{i+1}^{n+1}}=A_{4u_{i-1}^{n}}+A_{5u_i^{n}}+A_{6u_{i-1}^{n}}+P^* \quad (23)$$

Where, $A_1 = 2 - 3Zrh - 6r(1 + \beta)$, $A_2 = 8 + 12r(1 + \beta)$, $A_3 = 2 + 3Zrh - 6r(1 + \beta)$, $A_4 = 2 - 3Zrh + 6r(1 + \beta)$, $A_5 = 8 - 12r(1 + \beta)$, $A_6 = 2 + 3Zrh + 6r(1 + \beta)$,

$$P^* = 12Pk = 12k\frac{dU_\infty}{dt}+12k(Gr)\theta_i^j+24k\beta\left(\frac{\partial\omega^{(e)}}{\partial y}\right)$$

Similarly, the following system of equations is resolved by using the trapezoidal rule to equation 13 and applying the Crank-Nicholson technique.

$$B_1\ {}^{n+1}_{i-1}\ B\ u_2\ {}^{n+1}_{i}\ B\ u_3\ {}^{n+1}_{i+1}\ B\ u_4\ {}^{n}_{i-1}\ B\ u_5\ {}^{n}_{i}\ B\ u_6\ {}^{n}_{i+1} \quad (24)$$

Where, $B_1 = 2\eta - 3Zr\hbar\eta - 6r$, $B_2 = 8\eta + 12r$, $B_3 = 2\eta + 3Zr\hbar\eta - 6r$, $B_4 = 2\eta - 3Zr\hbar\eta + 6r$, $B_5 = 8\eta - 12r$, $B_6 = 2\eta + 3Zr\hbar\eta + 6r$.

Similarly, the following system of equations is resolved by using the trapezoidal rule to equation 14 and applying the Crank-Nicholson technique.

$$C_1\theta_{i-1}^{n+1}+C_2\theta_i^{n+1}+C_3\theta_{i+1}^{n+1}=C_4\theta_{i-1}^{n}+C_5\theta_i^{n}+C_6\theta_{i+1}^{n}+X^* \quad (25)$$

Where, $C_1 = 2(\mathrm{Pr}) - 3Zr\hbar(\mathrm{Pr}) - 6Wr$, $C_2 = 8(\mathrm{Pr}) + 12Wr$, $C_3 = 2(\mathrm{Pr}) + 3Zr\hbar(\mathrm{Pr}) - 6Wr$, $C_4 = 2(\mathrm{Pr}) - 3Zr\hbar(\mathrm{Pr}) + 6Wr$, $C_5 = 8(\mathrm{Pr}) - 12Wr$, $C_6 = 2(\mathrm{Pr}) + 3Zr\hbar(\mathrm{Pr}) + 6Wr$,

$$X^* = 12kX = 12kEc\left(\frac{\partial u^{(e)}}{\partial y}\right),\ W=\left(1+\frac{4}{3R}\right).$$

In this case, the mesh sizes along the y- and time-axes are h and k, respectively, and r = k/h2. The i, j terms are "space" and "time" are used in the index. In the equation 23, 24 and 25 taking $i = 1(1)n$ and using boundary conditions (13), then the set of equations below is found:

$$A_iX_i = B_i;\ i = 1(1)n \quad (26)$$

Where, $A_i^{'}$ s are order-n matrices and X_i, $B_i^{'}$ are an n-component column matrix.

The above system of equations is solved using the Thomas algorithm. MATLAB software is also used to find numerical solutions to these system equations. The MATLAB program proved the Galerkin finite element technique stability and convergence with smaller values of h and k, which also suggests small changes in the grades of u, ω, and θ. Hence the method Galerkin about finite elements, the result obtained was stable and convergent.

Results and Discussion

The goal of the current inquiry is to understand how radiation affects heat transfer in a moving, semi-infinite vertical porous plate and a micropolar fluid that is incompressible and viscous. All the way gives the analysis concerning numerical computations in temperature, velocity, and micro-rotation regions for different flow characteristics and conditions grades. In such a way, the boundary condition changed from y → ∞ to by $y = y_{max}$. Where 'y_{max}' is a far distance. For convenience, y_{max} = 12 we have chosen a step size of $\Delta y = 0.001$. In the boundary layer, with various values of Grashof number, the evaluated velocity profiles are shown in figure 2. The developed buoyancy force simulates a rise in the number of Grashof, increasing velocity grades.

The positive grades of Grashof number reveal the phenomenon of cooling on flow surface by convection. Inclusive of this, the curves in the figure indicate the velocity grades increase rapidly with the rash of number and then decay with fluid velocity. Without (Eckert number) viscous dissipation, the evolutions compared with the analytical results and observed that they are well verified (Figure 2). Figure 3 and figure 4 describes the influence of viscosity ratio on fluid micro-rotation and velocity profiles, respectively. Observed numerical results suggest deduced velocity grades are lower for a New-

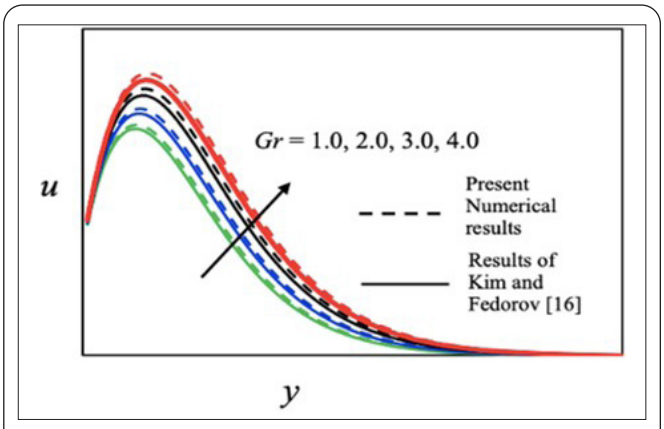

Figure 2: Analysis plot between analytical results to numerical velocity profiles results against spanwise 'y' coordinates with various Grashof number grades.

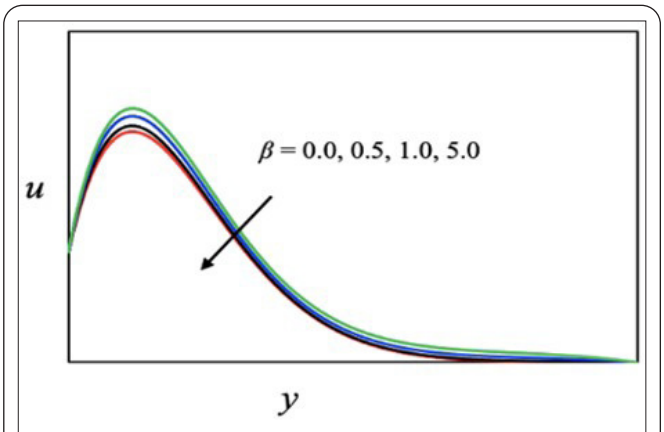

Figure 3: Variation in velocity against to the spanwise co-ordinate 'y' with various grades of β.

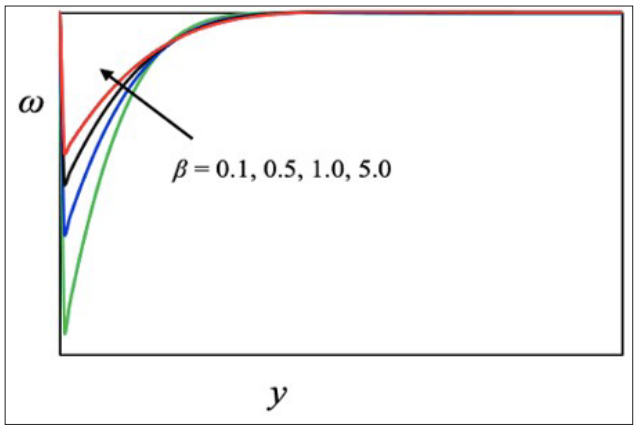

Figure 4: Variation in angular velocity to the spanwise co-ordinate 'y' with various grades of β.

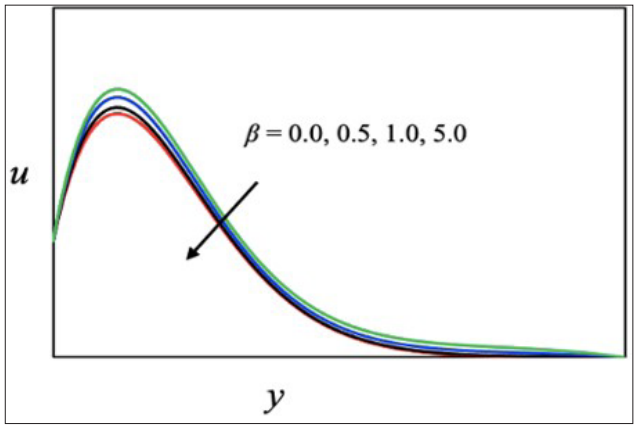

Figure 6: Variation in velocity profile to the spanwise co-ordinate 'y' with various grades of R.

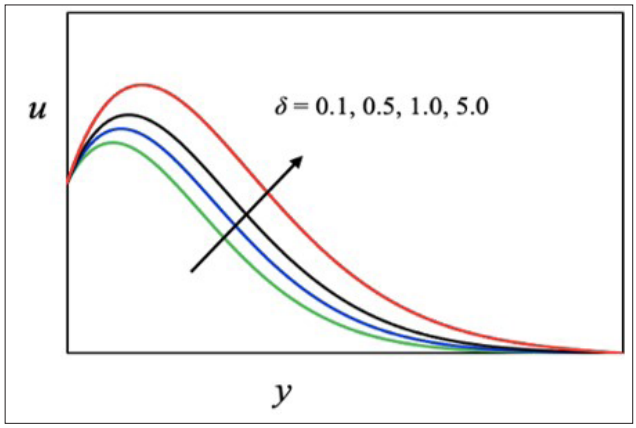

Figure 5: Variation in velocity profile to the spanwise co-ordinate 'y' with various grades of δ.

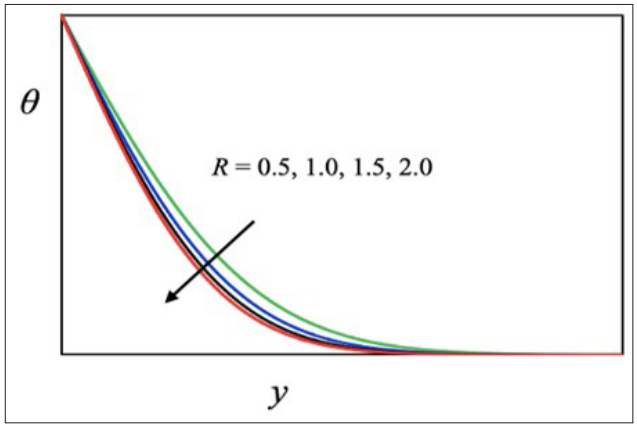

Figure 7: Variation in temperature profiles to the spanwise co-ordinate 'y' with various grades of R.

tonian fluid (β = 0). When viscosity ratios are less than one under similar flow properties and conditions. Once viscosity ratios are more than 1.0, velocity grades rapidly decrease. Including all, the additional distributions of micro-rotation do not exhibit differences in viscosity ratios. Figure 5 represents variation in velocity profiles to spanwise coordinate y for various grades of the parameter δ for micro-gyration vector. All the results suggest that the values of velocities increased with the δ-parameter It ultimately denotes free stream velocity at the boundary layer's edge. This change in velocity profile is expected as steam enters the turbulent phase, as shown by δ = 1.

Figure 6 and figure 7 represent the variation in the temperature and velocity profiles plotted against various radiation parameter values. The results all point to a reduction in velocity and temperature grades as the stream approaches its boundary layer due to increasing radiation parameter grades. In contrast, a decrease in the thickness of the stream will also affect both temperature and boundary layers. All the outcomes and results are due to enriched dominance of conduction over thermal radiation which lead to a decrease in buoyancy force in the stream with large R values and thickness of boundary layers. Figure 8 and figure 9 represents variation in Eckert number against velocity and temperature profiles with an influence of viscous parameter. The relationship between the stream's energy and enthalpy is described by the Eckert number, which also

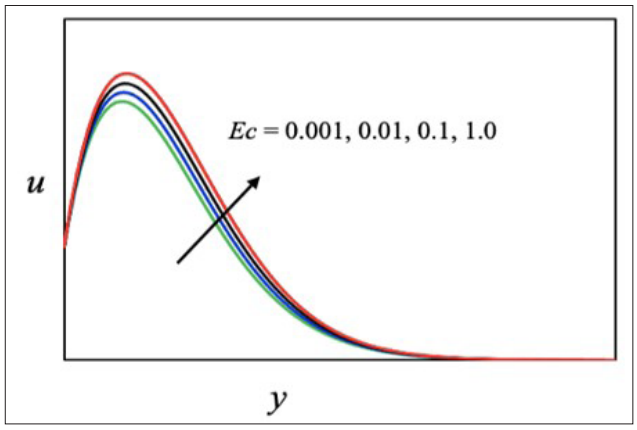

Figure 8: Variation in velocity profiles to the spanwise co-ordinate 'y' with various grades of E_c.

expresses the exchange of kinetic energy into internal energy against the stress of dense stream. More dissipative heat leads to an increase in both velocity and temperature. All the analyses observed represented both figure 8 and figure 9. Crucial changes in temperature grades concerning spanwise co-ordinate have represented in figure 10 with Prandtl number. All the numerical been represented an increase in Prandtl number grades, leading to a decrease in the thickness of the boundary

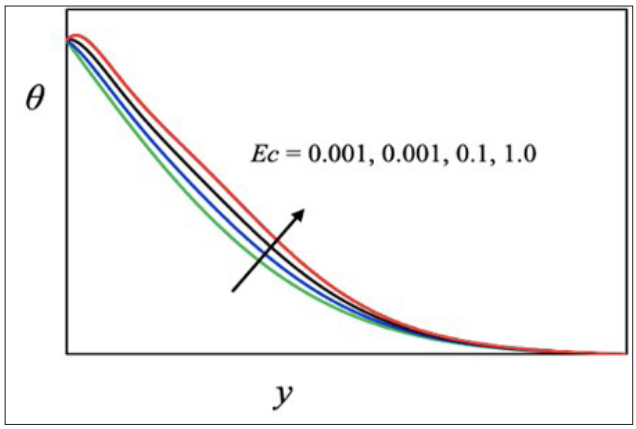

Figure 9: Variation in temperature profiles to the spanwise co-ordinate 'y' with various grades of E_c.

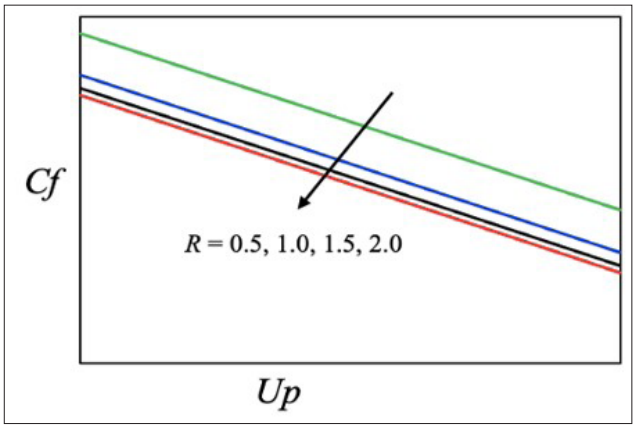

Figure 11: Influence of R (Thermal radiation parameter) on variation in skin-friction co-efficient against with U_p.

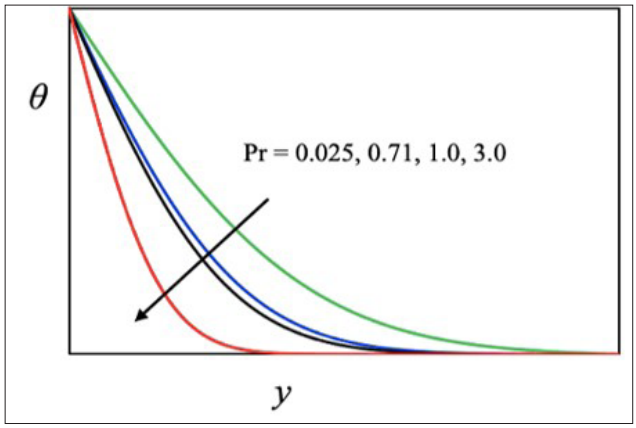

Figure 10: Variation in temperature profiles to the spanwise co-ordinate 'y' with various grades of Pr.

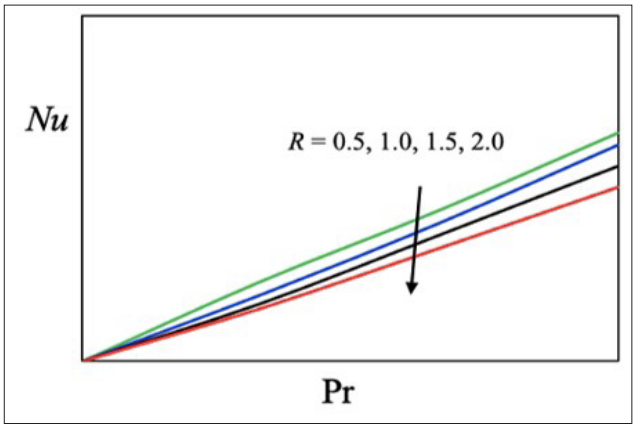

Figure 12: Influence of R (Thermal radiation parameter) on variation in Nusselt number against with the Pr.

layer. These are due to small grades of Pr influence the thermal conductivity of the stream, which further leads to more diffuse heat away from the surface apart from the grades Pr. Hence, one can conclude that a lower heat transfer rate was observed with a small Prandtl number around a thicker thermal boundary layer.

The observations from figure 11 suggest increased velocities of a porous plate in a stream of a present class lead to a linear decrease in values of skin friction with a decreased velocity gradient. In a particular case with a step size of R = 2.0, the observed surface skin friction coefficient is more than that of a step size of R = 1.0. These results reveal optimal conditions for the decrease in skin friction on the surface of the porous plate. Figure 12 describes the change in heat transfer concerning the radiative parameter with different grades of Prandtl number. Under necessary conditions and stream characteristics, the numerical results of the current problem suggest that surface heat transfer increases with increasing values of both Prandtl number and radiation parameter. All the outcomes (Table 1) of the present investigation are due to an increase in values of both Pr and R.

Table 1: Outcomes.

Cases	Parameters		Results, cm^{-2}
	f'	h''	
A	0.0	1.50	240.4161
B	1.0	4.50	229.348
C	2.0	85.00	562.179
D	0.0	23.50	516.527

Conclusion

Within this investigation, we have studied the uneven odd incompressible blended convection stream of micropolar thick dissipative molten past a semi-infinite porous plate. In which the porous plate introduced in the radiation field and its velocity kept constant. all of the problem analysis and resolution defined were done within the limits of the finite element technique. The results obtained are well analyzed and illustrated. All the stream details include heat transfer properties, various parameters, and their dependency on the stream boundaries and fluid characteristics. Radiation-dominated results were found to be better, and the radiation parameter 'R' is small. And the size of the thermal and momentum boundary layers is increasing. Which further leads to buoyancy-induced transport. And also decreases the heat transfer along with dimensional time at the boundary of the wall.

Additionally, the studies reveal a peak value of the radia-

tion parameter that affects the least friction at the top of the boundary wall. In the present investigation, increased stream velocity and temperature were due to originating viscous dissipation and increase in Eckert number. To better understand the current investigation, which includes overall stream mechanics and thermal behavior, one should perform prerequisite experimental tasks. In the coming years, we would be pleased to compare the obtained results with outcomes by upcoming researchers in the same field.

Acknowledgements

The author, T. Lokesh Babu thanks the administration of the Sreenidhi Institute of Science and Technology, Hyderabad, for giving the current investigation the necessary time and moral support.

Conflict of Interest

None.

References

1. Srinivasacharya D, Murthy JR, Venugopalam D. 2001. Unsteady stokes flow of micropolar fluid between two parallel porous plates. *Int J Eng Sci* 39(14): 1557-1563. https://doi.org/10.1016/S0020-7225(01)00027-1
2. Bhargava R, Kumar L, Takhar HS. 2003. Numerical solution of free convection MHD micropolar fluid flow between two parallel porous vertical plates. *Int J Eng Sci* 41(2): 123-136. https://doi.org/10.1016/S0020-7225(02)00157-X
3. Zueco J, Eguia P, Lopez-Ochoa LM, Collazo J, Patino D. 2009. Unsteady MHD free convection of a micropolar fluid between two parallel porous vertical walls with convection from the ambient. *Int Commun Heat Mass Transf* 36(3): 203-209. https://doi.org/10.1016/j.icheatmasstransfer.2008.11.008
4. Sheikholeslami M, Hatami M, Ganji DD. 2014. Micropolar fluid flow and heat transfer in a permeable channel using analytical method. *J Mol Liq* 194: 30-36. https://doi.org/10.1016/j.molliq.2014.01.005
5. Cheng CY. 2006. Fully developed natural convection heat and mass transfer of a micropolar fluid in a vertical channel with asymmetric wall temperatures and concentrations. *Int Commun Heat Mass Transf* 33(5): 627-635. https://doi.org/10.1016/j.icheatmasstransfer.2006.01.014
6. Kumar JP, Umavathi JC, Chamkha AJ, Pop I. 2010. Fully-developed free-convective flow of micropolar and viscous fluids in a vertical channel. *Appl Math Model* 34(5): 1175-1186. https://doi.org/10.1016/j.apm.2009.08.007
7. Umavathi JC, Sultana J. 2012. Mixed convective flow of a micropolar fluid mixture in a vertical channel with boundary conditions of the third kind. *J Eng Phys Thermophys* 85: 895-908. https://doi.org/10.1007/s10891-012-0728-4
8. Rahman MM, Aziz A, Al-Lawatia MA. 2010. Heat transfer in micropolar fluid along an inclined permeable plate with variable fluid properties. *Int J Therm Sci* 49(6): 993-1002. https://doi.org/10.1016/j.ijthermalsci.2010.01.002
9. Mahmoud MA. 2007. Thermal radiation effects on MHD flow of a micropolar fluid over a stretching surface with variable thermal conductivity. *Phys A Stat Mech Appl* 375(2): 401-410. https://doi.org/10.1016/j.physa.2006.09.010
10. Prasad VR, Vasu B, Bég OA, Parshad RD. 2012. Thermal radiation effects on magnetohydrodynamic free convection heat and mass transfer from a sphere in a variable porosity regime. *Commun Nonlinear Sci Numer Simul* 17(2): 654-671. https://doi.org/10.1016/j.cnsns.2011.04.033
11. Palani G, Kim KY. 2012. Influence of magnetic field and thermal radiation by natural convection past vertical cone subjected to variable surface heat flux. *Appl Math Mech* 33: 605-620. https://doi.org/10.1007/s10483-012-1574-7
12. Mahmoud MA, Waheed SE. 2012. Variable fluid properties and thermal radiation effects on flow and heat transfer in micropolar fluid film past moving permeable infinite flat plate with slip velocity. *Appl Math Mech* 33: 663-678. https://doi.org/10.1007/s10483-012-1578-x
13. Oahimire JI, Olajuwon BI. 2014. Effect of Hall current and thermal radiation on heat and mass transfer of a chemically reacting MHD flow of a micropolar fluid through a porous medium. *J King Saud Univ Eng Sci* 26(2): 112-121. https://doi.org/10.1016/j.jksues.2013.06.008
14. Kim YJ, Fedorov AG. 2003. Transient mixed radiative convection flow of a micropolar fluid past a moving, semi-infinite vertical porous plate. *Int J Heat Mass Transf* 46(10): 1751-1758. https://doi.org/10.1016/S0017-9310(02)00481-7
15. Rahman MM. 2009. Convective flows of micropolar fluids from radiate isothermal porous surfaces with viscous dissipation and Joule heating. *Commun Nonlinear Sci Numer Simul* 14(7): 3018-3030. https://doi.org/10.1016/j.cnsns.2008.11.010
16. Abd El-Aziz M. 2013. Mixed convection flow of a micropolar fluid from an unsteady stretching surface with viscous dissipation. *J Egypt Math Soc* 21(3): 385-394. https://doi.org/10.1016/j.joems.2013.02.010
17. El-Hakiem MA. 2000. Viscous dissipation effects on MHD free convection flow over a nonisothermal surface in a micropolar fluid. *Int Commun Heat Mass Transf* 27(4): 581-590. https://doi.org/10.1016/S0735-1933(00)00140-8
18. Eldabe NT, Ouaf ME. 2006. Chebyshev finite difference method for heat and mass transfer in a hydromagnetic flow of a micropolar fluid past a stretching surface with Ohmic heating and viscous dissipation. *Appl Math Comput* 177(2): 561-571. https://doi.org/10.1016/j.amc.2005.07.071
19. Rashad AM. 2009. Perturbation analysis of radiative effect on free convection flows in porous medium in the presence of pressure work and viscous dissipation. *Commun Nonlinear Sci Numer Simul* 14(1): 140-153. https://doi.org/10.1016/j.cnsns.2007.08.003
20. Eldabe NT, Sallam SN, Abou-zeid MY. 2012. Numerical study of viscous dissipation effect on free convection heat and mass transfer of MHD non-Newtonian fluid flow through a porous medium. *J Egypt Math Soc* 20(2): 139-151. https://doi.org/10.1016/j.joems.2012.08.013